J. Plasma Fusion Res. SERIES, Vol. 6 (2004) 527–530

Monte Carlo Simulation of Particle Transport in the LID Configuration

KANNO Ryutaro[1,2], JIMBO Shigeaki[2], TAKAMARU Hisanori[3] and OKAMOTO Masao[1,2]

[1]*National Institute for Fusion Science, Toki 509-5292, Japan*

[2]*Graduate University for Advanced Studies, Toki, 509-5292, Japan*

[3]*Department of Computer Science, Chubu University, Kasugai, 487-8501, Japan*

(Received: 9 December 2003 / Accepted: 23 February 2004)

Abstract

Monte Carlo simulation based on the test particle representation is carried out in order to understand the transport in the edge region of the Large Helical Device configuration with the Local Island Divertor (LID). It has the advantage of appropriately treating the collisionless edge plasma in the three-dimensional field line structure with the island and ergodic zones. The strike point pattern on the LID head is numerically observed under the effect of the Coulomb collisions, and the observations show that the pattern strongly depends on collisionless.

Keywords:

edge plasma transport, stochastic approach, Monte Carlo technique, Local Island Divertor, Large Helical Device

1. Introduction

Analyses of the edge plasma transport are classified to the fluid and particle representations. When collisionality is strong, it is known that the fluid approximation based on Braginskii's fluid equations is good enough [1,2]. If the high temperature divertor operation (HT-operation) is considered, there is a possibility to change this understanding, however.

The Local Island Divertor (LID) in the Large Helical Device (LHD) configuration [3,4] is one of the divertor concepts, and it utilizes an m/n=1/1 island formed at the edge region of the LHD. Control of the edge plasma by means of the LID is expected to realize the HT-operation.

In the HT-operation, the edge temperature is evaluated to be raised up to $\sim$ 5 keV by efficient pumping, thereby leading to enhancement in the energy confinement [4]. In this case, the edge plasma is collisionless, and the neo-classical effect on the transport becomes important.

Then, at first, in order to select the appropriate method solving the transport, we examine two stochastic approaches to the edge plasma transport, *i.e.* the fluid and test particle representations, in the three-dimensional (3-d) field line structure with the island and ergodic zones. After the examination of the approaches, the strike point pattern on the LID head is numerically observed by using a better way in the approaches.

2. Stochastic approach to edge plasma transport

2.1 Fluid representation

In studies of the edge plasma transport, a simplified fluid model is frequently employed [1]. The model is based on simplified Braginskii's fluid equations [1,2] neglecting the electric field and plasma current, *i.e.* a simple neutral plasma is assumed. The fluid equation for a fluid property f is given generally as

$$\frac{\partial f(\boldsymbol{x},t)}{\partial t} + \nabla\cdot\left[\boldsymbol{V}(\boldsymbol{x},t)f(\boldsymbol{x},t)\right] - \nabla\cdot\left[\overleftrightarrow{D}\cdot\nabla f(\boldsymbol{x},t)\right] = S(\boldsymbol{x},t), \quad (1)$$

where S is a source/sink of f and $\overleftrightarrow{D}$ is a tensor of a diffusion coefficient expressed as $\overleftrightarrow{D} = D_{\parallel}\,\boldsymbol{bb} + D_{\perp}\,(\overleftrightarrow{I} - \boldsymbol{bb})$. Here $\boldsymbol{b} = \boldsymbol{B}/|\boldsymbol{B}| = \boldsymbol{B}/B$ is a unit vector of a magnetic field $\boldsymbol{B}$ and $\overleftrightarrow{I}$ is the identity tensor. In order to solve directly the fluid equation (1), two kinds of differential operators along and across a field line, *i.e.* $\nabla_{\parallel}$ and $\nabla_{\perp}$, should be needed. It is not so easy to appropriately realize the operators in the 3-d field line structure with the island and ergodic zones.

Accordingly, one may consider that the Langevin equation can be used to solve the fluid equations, instead of directly solving them. In this case, the differential operators in the fluid equation (1) is represented by using the Langevin equation of a stochastic process $\boldsymbol{X}(t)$:

$$\mathrm{d}\boldsymbol{X}(t) = \left\{\boldsymbol{V}(\boldsymbol{X}(t),t) + \nabla\cdot\overleftrightarrow{D}(\boldsymbol{X}(t),t)\right\}\mathrm{d}t + \overleftrightarrow{\sigma}\cdot\mathrm{d}\boldsymbol{W}_t, \quad (2)$$

and the Langevin equation can be solved easily even in the 3-d field line structure, *e.g.* see refs. [5-7], where $\overleftrightarrow{\sigma} = \sqrt{D_{\parallel}}\,\boldsymbol{bb} + \sqrt{D_{\perp}}\left(\overleftrightarrow{I} - \boldsymbol{bb}\right)$ satisfies the condition $\mathrm{D}^{ij} = \sigma^{im}\sigma^{jn}g_{mn}$, g_{mn} is the metric coefficient, and $\boldsymbol{W}_t$

Corresponding author's e-mail: kanno@nifs.ac.jp

denotes a Wiener process. We will, however, find difficulty in the precision of the method based on the Langevin equation through the following discussion. For the simplicity of the discussion, we assume hereafter that the tensor $\vec{\vec{D}}$ is expressed as (1/2) $\vec{\vec{I}}$ and there is no source/sink, $S = 0$. When the fluid equation (1) is linear for f, the solution of eq. (1) with the initial condition $f(\boldsymbol{x}, 0) = \varphi(\boldsymbol{x})$ is given by using the Feynman-Kac (F-K) formula [8] as

$$f(\boldsymbol{x}, t) = \int \mathrm{d}y^3\, g(\boldsymbol{x}, t; \boldsymbol{y})\, \varphi(\boldsymbol{y}), \tag{3}$$

where the transition probability $g(\boldsymbol{x}, t; \boldsymbol{y})$ is expressed by the path integral:

$$g(\boldsymbol{x}, t; \boldsymbol{y}) = \int \mathcal{D}X \exp\left\{-\frac{1}{2}\int_0^t \mathrm{d}s \left[\frac{\mathrm{d}\boldsymbol{X}(s)}{\mathrm{d}s} - \boldsymbol{V}(\boldsymbol{X}(s), s)\right]^2\right\}. \tag{4}$$

Here a stochastic process $\boldsymbol{X}(t)$ starts from $\boldsymbol{X}(0) = \boldsymbol{y}$ and arrives at $\boldsymbol{X}(t) = \boldsymbol{x}$. If the trend term $\boldsymbol{V}$ is a mapping of the fluid property f itself, *i.e.* $\boldsymbol{V} = \boldsymbol{V}(f)$, then the fluid equation (1) becomes nonlinear, *e.g.* the Navier-Stokes (N-S) equation: $\boldsymbol{V} = \boldsymbol{f}$. When the F-K formula is stretched ad hoc in this case, the evolution of a fluid property f should be represented by using eq. (3): for n = 0, 1, 2, ···,

$$f^{(n+1)}(\boldsymbol{x}, t+\varepsilon) = \int \mathrm{d}y^3\, g^{(n)}(\boldsymbol{x}, t+\varepsilon; \boldsymbol{y}, t) f^{(n)}(\boldsymbol{y}, t), \tag{5}$$

and the transition probability is expressed as

$$g^{(n)}(\boldsymbol{x}, t+\varepsilon; \boldsymbol{y}, t) = \int \mathcal{D}X \exp\left\{-\frac{1}{2}\int_t^{t+\varepsilon} \mathrm{d}s \left[\frac{\mathrm{d}\boldsymbol{X}(s)}{\mathrm{d}s} - \boldsymbol{V}\left(f^{(n)}(\boldsymbol{X}(s), s)\right)\right]^2\right\}, \tag{6}$$

where the time interval ε is small enough compared with the time scale of interesting evolution of f, *i.e.* $O(\varepsilon) \ll O(1)$, but is large enough to sufficiently diffuse random walkers drawing the paths $\boldsymbol{X}(s)$: its mean square displacement is estimated as $\overline{(\delta x)^2} \sim O(\varepsilon)$. In the method, an error of the approximation is required to be always less than $O(\varepsilon)$. If an error of $\boldsymbol{f}$, $\boldsymbol{h}(\boldsymbol{x}, t)$ ordered as $|\boldsymbol{h}|/|\boldsymbol{f}| \sim O(\varepsilon)$, is caused, *i.e.* $\boldsymbol{f}^{(n)} = \boldsymbol{f} + \boldsymbol{h} = \boldsymbol{f}(1 + \varepsilon\hat{h})$, then we have the following estimation in the next step of the scheme (5);

$$\text{Equation (5)} \Rightarrow \frac{\partial \boldsymbol{f}}{\partial t} + \nabla\cdot\left[\boldsymbol{V}(\boldsymbol{f})\boldsymbol{f}\right] - \frac{1}{2}\Delta\boldsymbol{f} - \hat{h}\boldsymbol{f} + O(\varepsilon) + \cdots = 0. \tag{7}$$

Here, expanding eq. (5) to first order in ε, we have the differential equation (7). Therefore, in general it is not clear that the method can accurately treat the fluid equation with the nonlinear term.

In order to avoid this problem, one can use a stochastic variational method [9,10]. The scheme of this method is discussed in detail in ref. [10]. In the method, for example, we see that the variational principle of a functional $J[X]$ is equivalent to the N-S equation [9];

$$0 = \delta J[X] = \delta \int_0^t \mathrm{d}s\, E\left[\frac{1}{2}\left|DX(s)\right|^2\right] \Rightarrow \frac{\partial \boldsymbol{V}}{\partial t} + (\boldsymbol{V}\cdot\nabla)\boldsymbol{V} - \frac{1}{2}\Delta\boldsymbol{V} = -\frac{1}{\rho}\nabla p, \tag{8}$$

where $\mathrm{E}[\cdot]$ denotes a mathematical expectation based on the path integral (4), $\rho = \text{const}$ is the density, p is the pressure, and the mean forward derivative is defined as

$$DX(t) \equiv \lim_{\varepsilon\downarrow 0}\frac{1}{\varepsilon}\mathrm{E}[X(t+\varepsilon) - X(\mathrm{t})|X(t)] = \boldsymbol{V}(\boldsymbol{X}(\mathrm{t}), \mathrm{t}) \tag{9}$$

Here $\mathrm{E}[\cdot|\cdot]$ is a conditional expectation. According to the variational principle, if we find the process $X(t)$ giving the extremal value of the kinetic energy of fluid, then its trend term $\boldsymbol{V} = DX(t)$ is the solution of the N-S equation. But at present the stochastic variational method is restricted by severe conditions; *e.g.* an incompressible fluid should be considered, $\nabla\cdot\boldsymbol{V} = 0$ and $\rho = \text{const}$. Thus, the method needs the further extension. As a result of the above discussions, we find difficulty in the fluid representation of the edge plasma transport in the 3-d field line structure with the island and ergodic zones.

2.2 Test particle representation

In the test particle representation, there is no difficulty where we have seen in the previous subsection. We trace the orbits of the guiding centers in the fixed magnetic field under the effects of the collisions and the anomalous diffusion, in order to numerically observe the distribution of the guiding centers in the configuration space. If the effects of the collisions and the anomalous diffusion are neglected, the guiding center motion is expressed as [11]

$$\frac{\mathrm{d}\boldsymbol{X}}{\mathrm{d}t} = \boldsymbol{v} = \frac{1}{B_\parallel^*}\left[v_\parallel\left(\boldsymbol{B} + \frac{m_\alpha}{e_\alpha B}v_\parallel\nabla\times\boldsymbol{B}\right) + \left(\frac{\mu}{e_\alpha} + \frac{m_\alpha}{e_\alpha B}v_\parallel^2\right)\boldsymbol{b}\times\nabla B\right], \tag{10}$$

$$\frac{\mathrm{d}v_\parallel}{\mathrm{d}t} = -\frac{\mu}{m_\alpha B_\parallel^*}\left(\boldsymbol{B} + \frac{m_\alpha}{e_\alpha B}v_\parallel\nabla\times\boldsymbol{B}\right)\cdot\nabla B, \tag{11}$$

$$\frac{\mathrm{d}\mu}{\mathrm{d}t} = 0, \tag{12}$$

where $B_\parallel^* = B + (m_\alpha/e_\alpha B)v_\parallel \boldsymbol{b}\cdot\nabla\times\boldsymbol{B}$, $v_\parallel = \boldsymbol{v}\cdot\boldsymbol{b}$ is the parallel velocity, μ is the magnetic moment, and α is the species of the particle. Here we neglect the effect of the electric field. The Coulomb collision is expressed as [12]

$$\mathrm{d}\lambda = -\nu_d^{(\alpha)}\lambda\,\mathrm{d}t + \sqrt{(1-\lambda^2)\nu_d^{(\alpha)}}\,\mathrm{d}W_t^{(\lambda)}, \tag{13}$$

$$\mathrm{d}E = -2\nu_E^{(\alpha)}\left[E - \left(\frac{3}{2} + \frac{E}{\nu_E^{(\alpha)}}\frac{\mathrm{d}\nu_E^{(\alpha)}}{\mathrm{d}E}\right)T\right]\mathrm{d}t + \sqrt{4T_\alpha E\nu_E^{(\alpha)}}\,\mathrm{d}W_t^{(E)}, \tag{14}$$

where $\lambda = v_\parallel/|\boldsymbol{v}|$ is the cosine of the pitch angle, $E = (1/2)m_\alpha|v|^2$ is the energy of the particle, $\nu_d^{(\alpha)}$ is the deflection frequency, and $\nu_E^{(\alpha)}$ is the frequency of the energy scattering. The differential equations (10) - (14) are solved by using the Monte Carlo method [12]. When an ad hoc anomalous diffusion in the configuration space is considered, the motion in the configuration space is modified to the Langevin equation (2) with $\boldsymbol{V} = \boldsymbol{v}$ and $\vec{\vec{D}} = \vec{\vec{D}}_a$, where $\vec{\vec{D}}_a = D_a(\vec{\vec{I}} - \boldsymbol{bb})$ denotes the tensor of the anomalous diffusion.

If we want to accurately treat the evolution of the particle motions and the fields, of course we must select a particle simulation [13-15]. But it is highly time-consuming to solve all of the particle motions and the equations of the fields in the 3-d field line structure and in the interesting time scale. For the understanding of the edge plasma transport in the 3-d field line structure, the test particle representation has an advantage of relatively easily addressing it in spite of fixing the fields. As a result of the discussions, we can conclude that a better way is the test particle representation.

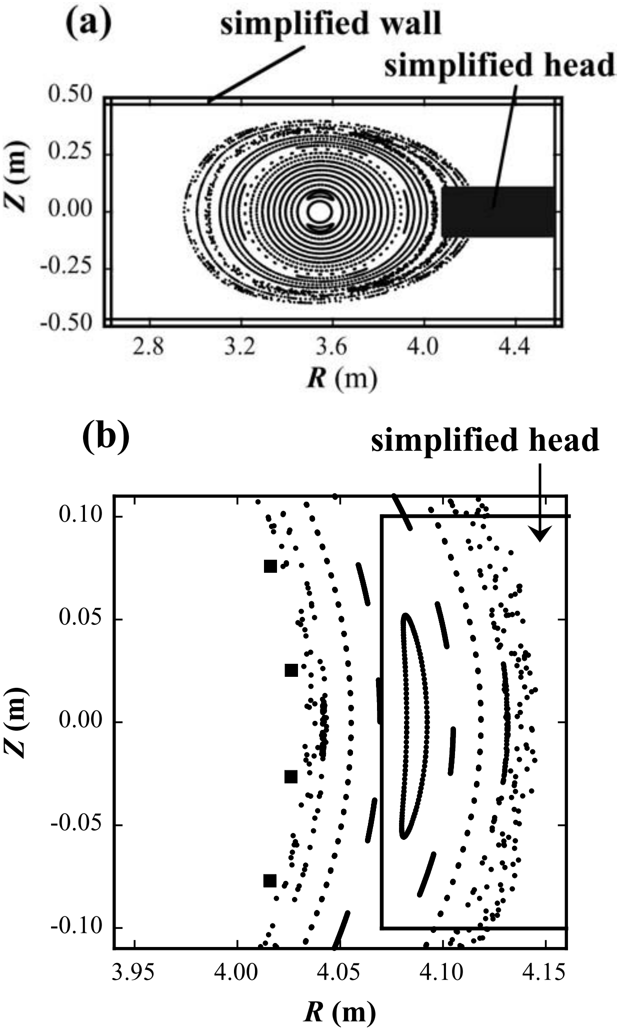

Fig. 1 (a) Poincaré plots of field lines of the vacuum magnetic field and sketch of the simplified LID head at the horizontally elongated poloidal cross section. The height of the head is 20 cm and the angle of the depth is 5.2 degrees. The magnetic axis and the O-point of the island are located at R_{ax} = 3.54 m and R_O = 4.09 m, respectively. (b) Expanded illustration of Fig. 1 (a). Field lines of the island are plotted by the dots, and the magnetic flux surface from which the test particles start is shown by the solid square.

2.3 Strike point pattern on LID head

By tracing the orbits of the guiding centers under the effect of the Coulomb collisions, the strike point pattern on the LID head is numerically observed. In this calculation, the shape of the head is simplified as a simple plate shown in Fig. 1. We use the vacuum magnetic field to calculate the orbits. We consider the situation that the test particles are mono-energetic protons with $E = 1$ keV, the distribution of the pitch angles is uniform at the start points of the particles, and the pitch angle scattering is dominant in collisions. We also assume that all of the particles start from the magnetic flux surface located at the edge of the core region, which is very close to the island separatrix (see Fig.1), and the particles are distributed uniformly on the surface. In this case, the width of the strike point pattern is evaluated as $\delta \sim 6$ cm, through the dimensional analysis: $|\boldsymbol{v}|/L \sim 4D_\perp/\delta^2$, where $L \sim 10^2$ m is the connection length between the edge of the core region and the LID head, and $D_\perp \sim 1\text{m}^2/\text{s}$ is a perpendicular diffusion coefficient guessed from the neo-classical coefficient in the core region for the collisionless regime.

When the collision frequency of the edge plasma is estimated as $\nu = 2 \times 10^5 \text{s}^{-1}$, we find that the strike point pattern is caused by the diffusion to the outside of the torus and it is not symmetric, as shown in Fig. 2. Here the test particles are assumed to be absorbed completely on the surface of the head. On the other hand, when the collision frequency is estimated as $\nu = 1 \times 10^3 \text{s}^{-1}$, the strike point pattern is drastically changed as shown in Fig. 3. The width of the pattern is measured as $\delta \sim 6$ cm. Comparison between the strike point patterns in Fig. 2 and 3 shows that for the collisional regime the orbits of the particles are not sensitive

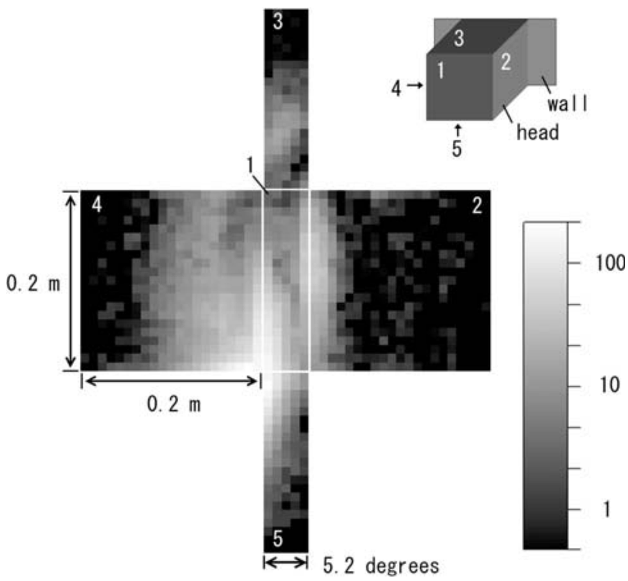

Fig. 2 Strike point pattern on the head for the collisional regime. The number of the particles is 2×10^4, and 55 % of them are absorbed into the head in this figure. The remaining particles are moving in the configuration space. The pattern is not symmetric on the surfaces of the head 2 and 4.

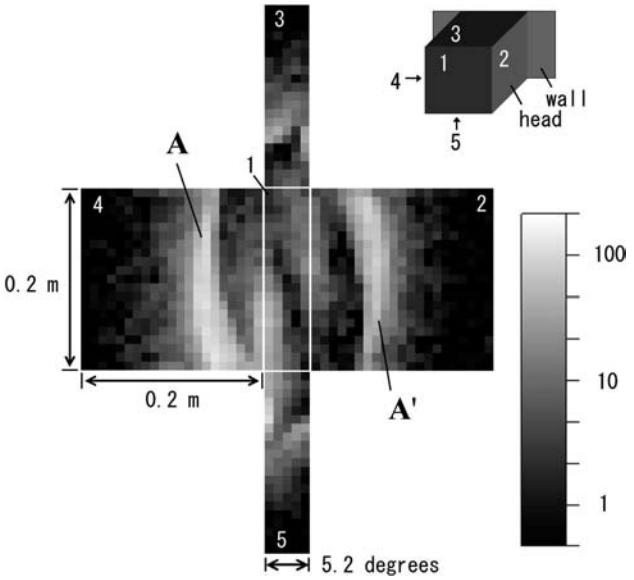

Fig. 3 Strike point pattern on the head for the collisionless regime. The number of the particles is 2×10^4, and 60 % of them are absorbed into the head in this figure. The remaining particles are moving in the configuration space. The regions of the pattern pointed by A and A′ are caused by the neo-classical diffusion.

to the field line structure of the island, however, for the collisionless regime the orbits are affected by the island structure and the pattern is caused by the neo-classical diffusion. The physical understanding of the strike point patterns, especially the understanding of the broken symmetry of the pattern in the collisional case, will be reported in detail in near future.

3. Conclusion

We have discussed the fluid and test particle representations of the edge plasma transport in the 3-d field line structure with the island and ergodic zones, and have shown the advantage of the particle representation. The strike point patterns on the simplified LID head have been numerically observed by tracing the orbits of the guiding centers in the fixed magnetic field under the effect of the Coulomb collisions. We have seen that the shape of the pattern strongly depends on the collision frequency.

In this article, we have neglected effects of electric field, energy scattering, anomalous diffusion, charge exchange, etc. These effects will be discussed in future work.

References

[1] P.C. Stangeby, *The Plasma Boundary of Magnetic Fusion Devices* (IOP, Bristol and Philadelphia, 2000).

[2] S.I. Braginskii, *Reviews of Plasma Physics, vol.1* (Consultants Bureau, New York 1965).

[3] A. Komori, N. Ohyabu *et al*., *Plasma Physics and Controlled Fusion Research*, (Vienna,1995).

[4] N. Ohyabu, A. Komori *et al*., J. Nucl. Mater. **220**, 298 (1995).

[5] Y. Feng, F. Sardei, J. Kisslinger and P. Grigull, J. Nucl. Mater. **241**, 930 (1997).

[6] Y. Feng, F. Sardei and J. Kisslinger, J. Nucl. Mater. **266**, 812 (1999).

[7] A.M. Runov, D. Reiter, S.V. Kasilov *et al*., Phys. Plasmas **8**, 916 (2001).

[8] I. Karatzas and S. E. Shreve, *Brownian Motion and Stochastic Calculus* (Springer, New York 1988).

[9] K. Yasue, J. Funct. Anal. **51**, 133 (1983).

[10] R. Kanno, J. Plasma Phys. **70**, 359 (2004).

[11] R.G. Littlejohn, J. Plasma Phys. **29**, 111 (1983).

[12] A.H. Boozer and G. Kuo-Petravic, Phys. Fluids **24**, 851 (1981).

[13] T. Takizuka and M. Hosokawa, Contrib. Plasma Phys. **40**, 471 (2000).

[14] T. Takizuka, M. Hosokawa and K. Shimizu, Fusion Technol. **39**, 111 (2001).

[15] T. Takizuka, M. Hosokawa and K. Shimizu, J. Nucl. Mater. **313-316**, 1331 (2003).